

08.78.19  
REPRINT

C. N. E. A. Biblioteca	
ARCHIVO PUBLICACIONES	
NO 1	AÑO 1978

ELSEVIER SEQUOIA S.A.  
Lausanne

AKADÉMIAI KIADÓ  
Budapest

EXCITATION FUNCTIONS AND THICK TARGET YIELDS FOR  
DEUTERON INDUCED REACTIONS ON ZIRCONIUM

C. Wasilevsky, F. Dos Santos, O. Herreros Usher, S. J. Nassiff

Comision Nacional de Energia Atomica, Buenos Aires, Argentina

Received 12 November 1977

Accepted 24 November 1977

Production cross sections of  $^{89}\text{Zr}$ ,  $^{97}\text{Zr}$ ,  $^{90\text{m}}\text{Y}$ ,  $^{90\text{g}}\text{Nb}$  and  $^{92}\text{Y}$  formed by the irradiation of natural zirconium with deuterons were measured. Thick-target yields for  $^{90}\text{Zr}$  (d,t)  $^{89}\text{Zr}$  reaction were determined for different irradiation times and as a function of de-  
uteron energy.

## INTRODUCTION

Many examples illustrate current trends in charged particles activation analysis which aims at further broadening and refining its capabilities, thus expanding its role as a tool for elemental trace and ultratrace analysis. The measurement of cross-sections are necessary in order to calculate the limits of detection for a given element in charged particles activation analysis<sup>1,2</sup>.

Such excitation functions are also crucial to the development of the field of radionuclide production by charged particle bombardment<sup>3</sup>.

Formation cross sections of residual nuclei produced by deuteron reactions change with the incident energy characteristically for the different processes involved. Although excitation functions do not lead to detailed understanding of nuclear reactions, they do contribute to the general picture of reaction mechanisms<sup>4</sup>.

This paper reports the experimental measurements of production cross sections of  $^{89}\text{gZr}$ ,  $^{97}\text{Zr}$ ,  $^{90\text{m}}\text{Y}$ ,  $^{90\text{g}}\text{Nb}$  and  $^{92}\text{Y}$  formed by irradiation of natural zirconium with deuterons. The results were compared with the data published by different authors<sup>5-9</sup> and with systematic studies<sup>10,11</sup>.

## EXPERIMENTAL

### Irradiations

Cross sections were measured by the activation method.

Stacks of zirconium foils were irradiated with the external beam of the Buenos Aires synchrocyclotron. The maximum uncertainty in the incident beam energy was estimated to be below 1%.

The targets were prepared with natural zirconium foils of high purity, provided by Koch Light Ltd. Their thickness was  $13 \text{ mg.cm}^{-2}$ . The target foils were placed between aluminium degrading foils of known thicknesses.

The energy of deuterons at the middle of each target foil of the stack was determined from the tables of Williamson, Boujot and Picard<sup>12</sup>. The energy straggling in the target was estimated to be about 0.5 MeV for the foil in which the deuterons had been slowed down to 16 MeV<sup>13</sup>.

Since the excitation function of the  $^{27}\text{Al} (d, \alpha p) ^{24}\text{Na}$  reaction<sup>14</sup> is well known, the yield of radioactive isotopes in the zirconium foils relative to that of  $^{24}\text{Na}$  in the aluminum foils provides a means for obtaining absolute cross sections for the deuteron reactions on zirconium.

### Counting

After bombardment, the gamma spectra of each sample were measured without previous chemical separation using a high resolution Ge(Li) detector connected to a multichannel pulse-height analyzer. The absolute detection efficiency was determined with calibrated sources of known activity.

Several efficiency determinations agreed within the statistical error of 1%. The formula  $\varepsilon(E_{\gamma}) = \text{const. } E_{\gamma}^{-n}$  was used to interpolate the efficiency  $\varepsilon(E_{\gamma})$  to other energies.

The nuclides produced by deuteron induced reactions were recognized by carefully following of the decay curves at each photopeak energy.

The photopeak areas were calculated by using Wasson's method<sup>15-16</sup>. The relative activities at the end of the irradiations were calculated extrapolation of the decay curves. The detector efficiency and decay scheme data<sup>17,18</sup> were used to convert peak area to absolute activity of each radioisotope. These data with those of the flux, were employed to calculate the production cross sections for the nuclides observed in each foil.

Corrections for the energy spread in each foil due to uncertainties in the foil thickness and the energy decrease in the preceding foils, were not applied. Losses of reaction products by recoil were assumed to be negligible.

## RESULTS AND CONCLUSION

The cross sections and excitation functions for the production of radioisotopes measured in the present work are shown in Figs 1 to 5.

The maximum error in the determination of the cross sections is estimated to be below 15%.

Since the radiochemical technique deals only with the residual nuclei, and not the emitted particles, it cannot, in itself, distinguish neither the reaction modes nor the different reactions producing the same nuclide when these are energetically possible and the threshold differences are not appreciable. For example (d, t) means (d, t) (d, p2n) or (d, dn).

The production cross sections measured are not always corrected for the atomic weight and the isotopic abundance of each target nuclide principally when several reactions starting from different zirconium isotopes con-

TABLE 1

Cross sections for the production of nuclides by deuteron induced reaction on zirconium.

$E_d$ (MeV)	$\bar{\sigma}$ (mb)		$\bar{\sigma}_p$ (mb)	$\bar{\sigma}_p$ (mb)	$\Sigma a_i / \bar{A}$ $^{92}_{\text{Y}}$
	$^{89}_{\text{Zr}}$	$^{97}_{\text{Zr}}$	$^{90}_{\text{mY}}$	$^{90}_{\text{gNb}}$	
25.3		207.0		4.318	0.058
25.0	151.0	180.0		4.088	0.044
24.6	183.0	168.0		4.934	0.054
23.5	145.0	173.0		5.519	0.051
22.8		192.0		5.780	0.050
22.0	132.0	214.0		5.945	0.049
21.2	67.8	192.0	18.8	6.275	0.053
20.5		217.0	18.9	5.879	0.056
19.7		235.0	17.5	5.945	0.057
18.8	18.8	220.0	17.6	5.791	0.054
17.9	17.7	242.0			0.058
16.9	17.0		17.0	5.648	0.052
15.9	7.1	227.0	17.4	5.560	0.053
14.9		234.0		4.714	0.059
13.8		241.0	16.4	3.417	0.052
12.6		264.0		2.121	0.049
11.3		194.0	15.3	0.225	0.035
9.5		121.0			0.019
8.3		88.0	9.7		0.014
7.3		58.0			0.007
6.1		5.6	3.0		

tribute to the formation of a given product nuclide. To evaluate these contributions the shapes of the excitation functions given by Lange and Münzel in their systematic work<sup>10</sup> were considered, taking into account the threshold energies.

The excitation functions may in some instances include contributions from the decay of short-lived precursors.

$^{89g}\text{Zr}$  directly produced by  $^{90}\text{Zr}(d, t)^{89g}\text{Zr}$  (Fig. 1) would be partially generated by  $^{89m}\text{Zr}$  and by  $^{89m/g}\text{Nb}$  and therefore they would contribute to the measured yield of  $^{89}\text{Zr}$ . The half-life of  $^{89m}\text{Zr}$  is 4.18 m, and those

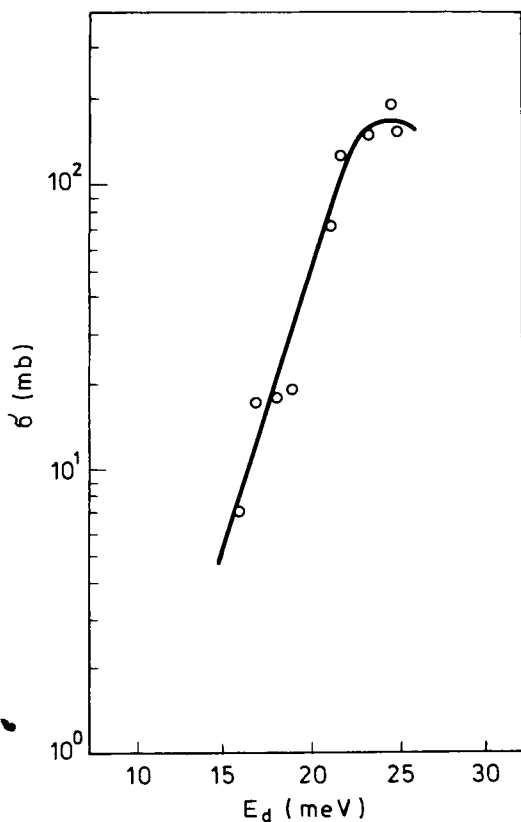


Fig. 1. Excitation function for the  $^{90}\text{Zr}(d, t)^{89g}\text{Zr}$  reaction. Correction for the isotopic abundance of  $^{90}\text{Zr}$  (0.5146) was already applied

of  $^{89m}\text{Nb}$  and  $^{89g}\text{Nb}$  are respectively 2.03 h., and 1.1 h; that is, the  $^{89m}\text{Zr}$  and  $^{89m/g}\text{Nb}$  produced during bombardments will be detected as  $^{89g}\text{Zr}$  in spectra measured several hours or days after the bombardments.

No previously published (d, t) excitation function on  $^{90}\text{Zr}$  is known.

In Fig. 2 is drawn the excitation function for the  $^{96}\text{Zr}(d, p)^{97}\text{Zr}$  reaction obtained in the present work and is confronted with the results observed by Otozai et al.<sup>8</sup> and Bock<sup>9</sup>.

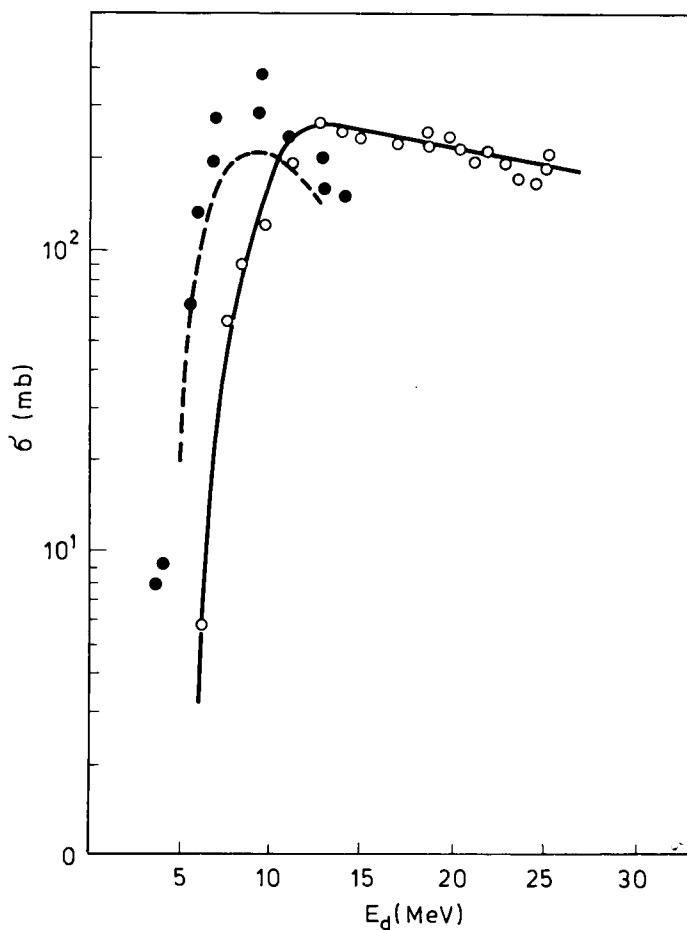


Fig. 2. Excitation function for the  $^{96}\text{Zr}(d, p)^{97}\text{Zr}$  reaction. ●●●Otozai et al.<sup>8</sup> --- Bock<sup>9</sup>

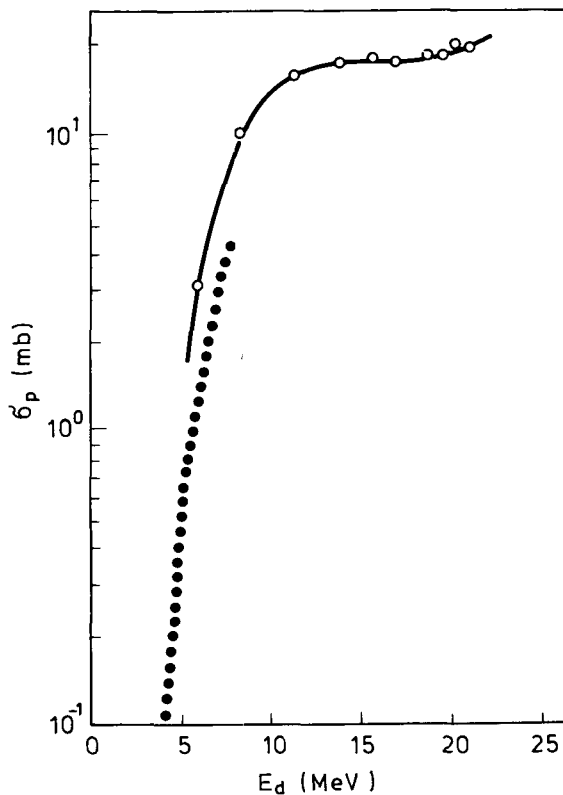


Fig. 3. Production cross-sections for  $^{90m}\text{Y}$ . . . . Excitation function for the  $^{92}\text{Zr}(d,\alpha)^{90m}\text{Y}$  ooo reaction published by Anders and Meinke<sup>7</sup>

Fig. 3 shows the  $\sigma_p$  values obtained in the present work for the production of  $^{90m}\text{Y}$ . It should be taken into account that the atomic weight was considered as:

$$\bar{A} = \frac{\sum_i A_i a_i}{\sum_i a_i}$$

and the isotopic abundance as  $\sum_i a_i$  where  $A_i$  and  $a_i$  are, respectively, the atomic weight and the isotopic abundance of the target nuclides, of those involved in the residual nucleus production.

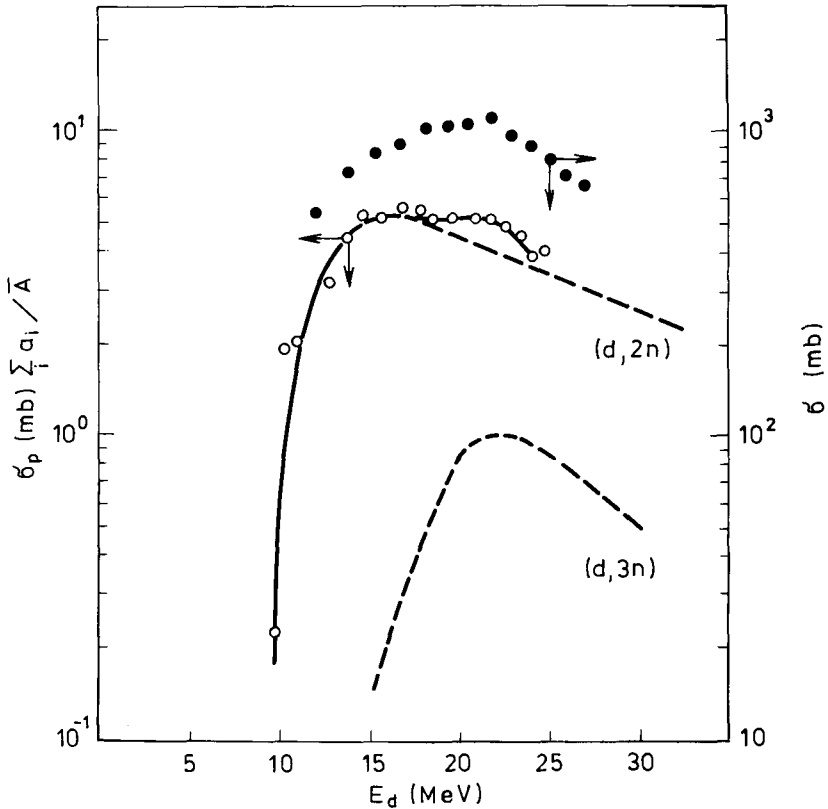


Fig. 4.  $\sigma_p(\text{mb}) \sum_i a_i / \bar{A}$  for  $^{90g}\text{Nb}$  formation. Dashed lines represent the estimates of different possible reactions. ●●● Mercader et al.<sup>5</sup>

Contributions from  $^{90}\text{Zr}(d, 2p)$ ,  $^{91}\text{Zr}(d, 2pn)$ ,  $^{92}\text{Zr}(d, 2p2n)$  and  $^{92}\text{Zr}(d, \alpha)$  reactions were not estimated. The present work data and the reported values by Anders and Meinke<sup>7</sup> are compared.

Fig. 4 shows  $\sigma_p(\text{mb}) \sum_i a_i / \bar{A}$  for  $^{90g}\text{Nb}$ . In the energy interval considered  $^{90g}\text{Nb}$  is produced by disintegration of  $^{90m}\text{Nb}$  (18.8 s) and by the following reactions:  $^{90}\text{Zr}(d, 2n)$ ,  $^{91}\text{Zr}(d, 3n)$  and  $^{92}\text{Zr}(d, 4n)$ , the thresholds energies being 9.50 MeV, 16.66 MeV and 25.81 MeV, respectively. The excitation functions shown as dashed curves, represent estimates of the contributions of the different possible reactions. Cross points denote

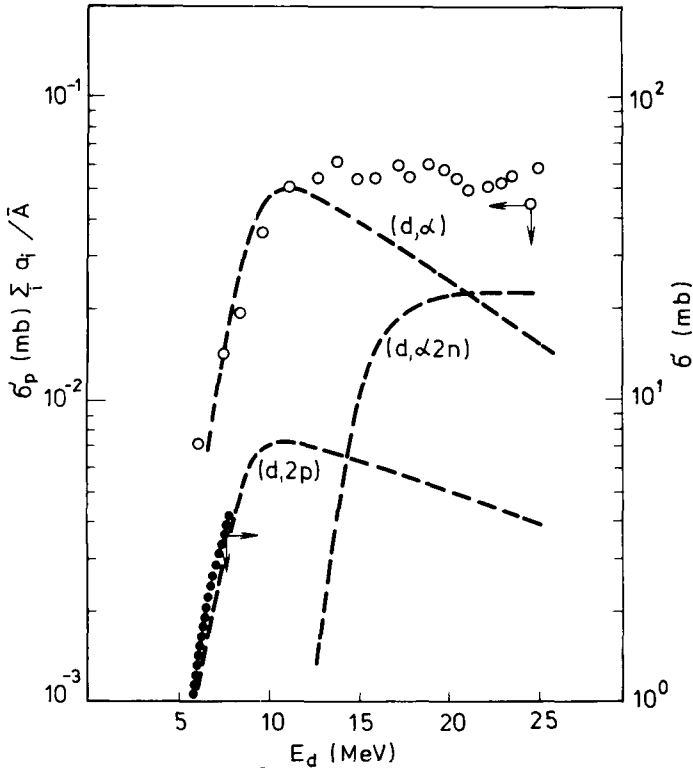


Fig. 5.  $\sigma_p(\text{mb}) \sum_i a_i / \bar{A}$  for  $^{92}\text{Y}$  formation. Dashed lines represent the estimates of different possible reactions. Points line shows the  $^{94}\text{Zr}(d,\alpha)^{92}\text{Y}$  excitation function published by Anders and Meinke<sup>7</sup>

the results reported by different authors<sup>5</sup>. If a correction due to relative abundances of  $^{90}\text{Zr}$  and  $^{91}\text{Zr}$  isotopes is applied, the results agree.

Experimental  $\sigma_p(\text{mb}) \sum_i a_i / \bar{A}$  for the  $^{92}\text{Y}$  formation is drawn in Fig. 5. Dashed curves are an estimation of contributions of  $^{94}\text{Zr}(d,\alpha)$ ,  $^{92}\text{Zr}(d,2p)$  and  $^{96}\text{Zr}(d,\alpha 2n)$  reactions with thresholds energies of 0.0 MeV, 5.2 MeV and 6.1 MeV, respectively. The excitation function of the  $^{94}\text{Zr}(d,\alpha)^{92}\text{Y}$  reaction, published by Anders and Meinke<sup>7</sup> is represented as a pointed line.

The maximum cross sections calculated with the values obtained from our data were compared, when possible, with published excitation functions<sup>10,11</sup>, showing a good agreement.

TABLE 2

Energy range (MeV)	Thickness of the target (mg/cm <sup>2</sup> )	Cross section (m. b.)	Saturation activity ( $\mu\text{Ci}/\mu\text{A}$ )	$\Sigma$ Saturation activity ( $\mu\text{Ci}/\mu\text{A}$ )	$\Sigma A_t / 10$ ( $\mu\text{Ci}/\mu\text{A}$ )	$\Sigma A_{1h}$ ( $\mu\text{Ci}/\mu\text{Ah}$ )
25-24	48.3	164	$1.6014 \times 10^3$	$1.7623 \times 10^4$	$1.1802 \times 10^3$	$1.5506 \times 10^2$
24-23	46.9	152	$4.141 \times 10^3$	$1.3022 \times 10^4$	$8.7204 \times 10^2$	$1.1455 \times 10^2$
23-22	45.4	130	$3.432 \times 10^3$	$8.8810 \times 10^3$	$5.9473 \times 10^2$	$7.8097 \times 10$
22-21	43.9	85	$2.170 \times 10^3$	$5.4490 \times 10^3$	$3.6490 \times 10^2$	$4.7914 \times 10$
21-20	42.5	54	$1.335 \times 10^3$	$3.2790 \times 10^3$	$2.1958 \times 10^2$	$2.8831 \times 10$
20-19	40.9	35	$8.327 \times 10^2$	$1.9440 \times 10^3$	$1.3018 \times 10^2$	$1.7094 \times 10$
19-18	39.5	22	$5.055 \times 10^2$	$1.1113 \times 10^3$	$7.442 \times 10^1$	9.7730
18-17	37.9	16	$3.527 \times 10^2$	$6.058 \times 10^2$	$4.057 \times 10^1$	5.3289
17-16	36.3	12	$2.531 \times 10^2$	$2.531 \times 10^2$	$1.695 \times 10^1$	2.2277

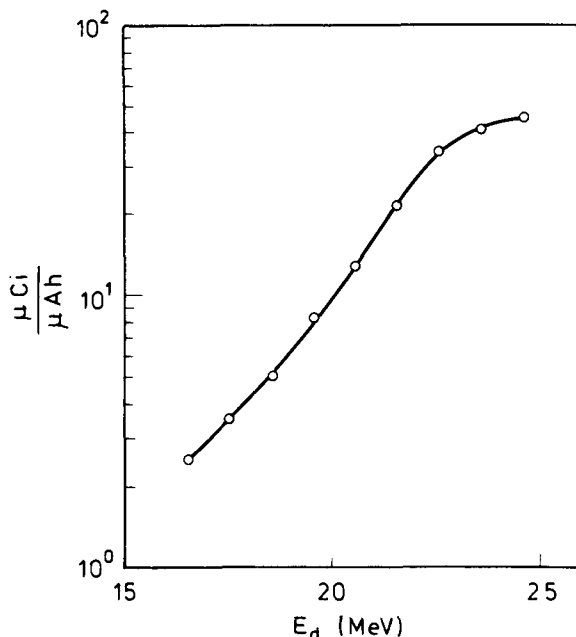


Fig. 6. Thick-target yields for the  $^{90}\text{Zr}(d, t)^{89}\text{Zr}$  reaction

It is not intended to clarify the reaction mechanisms for the presented excitation functions in the frame of this work.

The thick target yields for the formation of  $^{89g}\text{Zr}$  have been calculated by numerical integration using the experimental values of cross sections obtained in the present work with the method proposed by Svoboda<sup>3,10</sup>. The values are plotted on Fig. 6. It should be taken into account that the isotopic abundance was considered 0.5146 for the evaluation of thick target yields.

✱

The authors are indebted to the Synchrocyclotron staff who performed the irradiations, and Mr. Remigio Fontanille for his assistance and cooperation. The kind help in allowing to use the equipments is gratefully acknowledged to Miss Maria del Carmen Rotta.

REFERENCES

1. K. Svoboda, D. J. Silvester, Int. Journ. of Appl. Rad. and Isotop. 23 (1972) 203.
2. E. A. Schweikert, J. R. Mc Ginley, J. J. Stock, Transactions of the American Nuclear Society, International Nuclear and Atomic Activation Analysis Conference and Nineteenth Annual Meeting on Analytical Chemistry in Nuclear Technology; October 14-16, 1975, Gatlinburg, Tennessee.
3. K. Svoboda, Ľ. J. V. Report 2258 Ch, Czechoslovakia, 1969.
4. H. F. Röhm, K. A. Keller, H. Münzel, KFK 1730, Kernforschungszentrum, Karlsruhe, 1973.
5. R. C. Mercader, M. C. Caracoche, A. B. Mocoroa, Z. Physik, 255 (1972) 103.
6. O. U. Anders, AECU- 3513, 1957.
7. O. U. Anders, W. Meinke, Phys. Rev. 120 (1960) 2114.
8. K. Otozai, S. Kuze, H. Okamura, A. Mito: Nucl. Phys. A 107 (1968) 427.
9. R. Bock, Z. Physik 164 (1961) 548.
10. J. Lange, H. Münzel, Report KFK 767, Kernforschungszentrum, Karlsruhe, 1968.
11. K. A. Keller, J. Lange, H. Münzel, G. Pfennig, Landolt-Börstein, Numerical Data and Functional Relationships in Science and Technology, Vol. 5, part. b, 1973 and part. c, 1974.
12. C. F. Williamson, J. P. Boujot, J. Picard, Rapport CEA-R 3042.
13. S. M. Seltzer, M. J. Berger, Report NAS-NRC, Publ. 1133; Nucl. Sci. Series Report Nr. 39, 1964.
14. U. Martens, G. M. Schweimer, Report KFK 1083, Kernforschungszentrum, Karlsruhe, 1969.

15. P. A. Baedeker, Anal. Chem., 43 (1971) 405.
16. S. Taczanowski, ITJ N<sup>o</sup> 37/I, 1973.
17. C. M. Lederer, J. M. Hollander, I. Perlman, Table of Isotopes, Wiley and Sons, New York, 1967.
18. Nuclear Data Sheets, National Academy of Sciences.